Volume 15 Issue 5 May 2007 ISSN 0967-0661

ELSEVIER

CONTROL ENGINEERING PRACTICE

A Journal of IFAC the International Federation of Automatic Control

CONTENTS

Continued on back cover

Available online at
ScienceDirect
www.sciencedirect.com

IFAC

Available online at www.sciencedirect.com
ScienceDirect
Control Engineering Practice 15 (2007) 511–519
CONTROL ENGINEERING PRACTICE
www.elsevier.com/locate/conengprac

Optimal cruise control of heavy-haul trains equipped with electronically controlled pneumatic brake systems☆

M. Chou, X. Xia*

Department of Electrical, Electronic and Computer Engineering, University of Pretoria, Pretoria, 0002, South Africa

Received 3 August 2005; accepted 11 September 2006
Available online 27 October 2006

Abstract

A closed-loop cruise controller is proposed to minimise the running cost of heavy-haul trains equipped with electronically controlled pneumatic brake systems. Consideration is given to improving velocity tracking, in-train force management and energy usage. To overcome the communication constraints, a fencing concept is introduced, whereby the controller reconfigures adaptively to the current track topology. Simulation results of comparisons between different controllers are provided: open-loop versus closed-loop; velocity tracking versus in-train force. Different train control configurations are also compared: unified control, adaptive fencing and full independent traction and braking.

Keywords: Closed-loop; Cruise control; Electronically controlled pneumatic (ECP) brake system; Heavy-haul train; LQR; Optimal control

1. Introduction

Optimisation objectives are one of the key parameters in controller design. In heavy-haul trains, optimal control entails minimising operational cost while arriving at the destination within the required time frame.

The three main factors contributing to the running cost of heavy-haul trains are energy consumption, travelling time and maintenance: energy consumption is directly proportional to the amount of control action used; extended travelling time results in heavy fines charged by the client for late deliveries, especially in the case of port export; maintenance and repair of damage to the brake and coupler system, mainly caused by excess in-train forces in long heavy-haul trains, are expensive.

In this paper, control methods for both passenger and heavy-haul trains are examined. An optimal cruise controller is designed for heavy-haul trains equipped with electronically controlled pneumatic (ECP) brake systems. The controller design is based on a longitudinal dynamical model proposed and validated against real data in the companion paper (Chou, Xia, & Kayser, 2006).

The controller is tested on this model as well. The performance of different controller configurations, as well as the effects of individual control over unified control, is compared. Three controller configurations are considered: velocity tracking emphasised controller, in-train forces emphasised controller and energy usage emphasised controller. A unified braking and traction controlled train is compared with a full individual brake and traction controlled train. The performance indices are velocity deviation, maximum in-train forces and energy usage.

This paper describes the controller design process in four main steps: description of existing methods, a brief description of the model, controller design and results.

2. Control methods

Energy efficiency comes first, maybe indirectly, from optimal local control of traction, braking and more recently active steering and suspension. An example is the slip controller. Maintaining maximum slip improves tractive efforts, hence reduces energy consumption. To achieve this, an accurate measurement of the wheel velocity

☆A preliminary version of the paper was presented at the 16th IFAC World Congress held in Prague, 4–8 July 2005.

*Corresponding author. Tel.: +27 12 420 2165; fax: +27 12 362 5000.
E-mail address: xxia@postino.up.ac.za (X. Xia).

0967-0661/$ - see front matter
doi:10.1016/j.conengprac.2006.09.007

is required. This is difficult and expensive owing to the harsh environment found at the under-carriage. A novel wheel slip detector via the measurement of the traction motor current changes was shown by Watanabe and Yamashita (2001), while Ishikawa and Kawamura (1997) demonstrated a PI-based controller that is able to maintain the slip velocity very closely around the optimal point with minimum jittering.

Another example is the mechatronic control system for passenger trains equipped with actively controlled suspension (Goodall & Kortum, 2002; Mei, Nagy, Goodall, & Wickens, 2002). Bogie[1]-based control methods for steering and stability are proposed by Pearson, Goodall, Mei, and Himmelstein (2004) and Perez, Busturia, and Goodall (2002).

These studies offer some insights into train dynamics. However, these control methods require new vehicles because of the extensive use of advance actuators. Moreover, these controllers focus on the ride quality of the trip, a minor concern in heavy-haul trains.

On the train operational level, an energy efficient controller uses optimal scheduling. Howlett (1996) and Howlett, Milroy, and Pudney (1994) proposed such a controller for a diesel-powered passenger train that is able to reduce energy consumption while completing the journey within a certain time limit. A similar method was also proposed by Khmelnitsky (2000).

In practice optimal scheduling suffers from some deficiencies. These studies use a point-mass model, ignoring the in-train dynamics. Scheduling predetermines the control strategies under an assumed condition. Lengthy recalculation will have to be performed if disturbances are present. Possible scenarios include stopping for additional wagons to be attached and emergency stops. Unpredictable factors such as weather conditions will also affect the performance of the optimal strategy.

Automatic speed controllers discussed by Thelen and Tse (1990) and Tang and Gao (1996) are examples of the handling of in-train forces. The controllers calculate the optimal speed profile the train should adhere to before reaching its stop. These studies conclude that by following a smooth speed profile, extreme control force are avoided while minimising in-train forces. However, these studies are limited to the stopping of the train.

More recently, Yang and Sun (2001) discussed the use of the H_2/H_∞ control method for the cruising of a high-speed passenger train. The main improvement was the disturbance rejection property and the use of a spring-mass model. Astolfi and Menini (2002) explored the decoupling property of the model proposed by Yang and Sun (2001).

Point-mass models used by previous heavy-haul train studies ignore in-train dynamics. In comparison, a spring-mass model considers the train as individual masses that are inter-connected via spring-like couplers. This allows the in-train dynamics to be analysed.

[1]The suspension system including wheel set(s).

In heavy-haul trains, the use of a spring-mass model was hindered by the use of pneumatically controlled brakes. The slow propagating pneumatic signal poses a delay problem in heavy-haul trains, which could extend over 2.5 km or longer. The result is uneven braking throughout the train. In earlier studies, such complex dynamics was neglected. An example is the suboptimal control proposed by Gruber and Bayoumi (1982). In that paper, other simplifications were made to reduce overall train length by considering only the rear coupler of each car. Without model validation, it is difficult to evaluate the practicality of the proposed controller.

The introduction of the ECP brake system (Kull, 2001; Hawthorne, 2003) solves the dilemma. Electronic control signals allow simultaneous braking throughout the train as well as individual braking of each wagon and locomotive. A longitudinal dynamical model of heavy-haul trains equipped with ECP was proposed and validated in Chou et al. (2006).

Two issues need to be addressed before an ECP system can improve operational efficiency. Firstly, fully individual brake control is limited by computation and bandwidth constraints. In the specification by AAR (2002), a maximum of 32 control channels is specified. With a typical heavy-haul train consisting of 200 wagons, individual control is currently not possible. Secondly, the existing controller does not take advantage of the additional control inputs.

In this study, adaptive grouping, termed adaptive wagon fencing, is used to tackle the bandwidth problem: cars experiencing a similar track environment are controlled as a group, reducing the required control signals and thus the bandwidth requirement.

The second issue is that existing controllers do not utilise the additional control inputs. In this study, the cruise controller is designed generically so it can adapt to different train configurations in terms of a varying number of locomotives and wagons and their placements. This allows the controller to take advantage of the ECP technology.

3. Train model

In the proposed model, equations of motion are used to describe the longitudinal motion of the train. Through coupler forces, the in-train dynamics is examined. Rolling resistance and aerodynamic resistances, as well as gravitational and curvature resistances, are considered. Of the four, gravitational resistance is the largest.

For details of the modelling, refer to Chou et al. (2006). Equations of motion are included in the following for completeness:

$$\begin{aligned} m_1\ddot{x}_1 &= u_1 - k_1(x_1 - x_2) - d_1(\dot{x}_1 - \dot{x}_2) \\ &\quad - (c_0 + c_v\dot{x}_1)m_1 - c_a\dot{x}_1^2\left(\sum_{i=1}^{n} m_i\right) \\ &\quad - 9.98\sin\theta_1 m_1 - 0.004D_1m_1, \end{aligned}$$

$$\begin{aligned} m_i\ddot{x}_i = {} & u_i - k_i(x_i - x_{i+1}) - k_{i-1}(x_i - x_{i-1}) \\ & - d_i(\dot{x}_i - \dot{x}_{i+1}) - d_{i-1}(\dot{x}_i - \dot{x}_{i-1}) \\ & - (c_0 + c_v\dot{x}_i)m_i - 9.98\sin\theta_i m_i \\ & - 0.004D_i m_i, \quad i = 2, \ldots, n-1, \end{aligned} \tag{1}$$

$$\begin{aligned} m_n\ddot{x}_n = {} & u_n - k_{n-1}(x_n - x_{n-1}) \\ & - d_{n-1}(\dot{x}_n - \dot{x}_{n-1}) - (c_0 + c_v\dot{x}_n)m_n \\ & - 9.98\sin\theta_n m_n - 0.004D_n m_n, \end{aligned}$$

where, n is the number of units, i.e., rakes and locomotives, $\dot{x}_i$ and x_i are the velocity and the displacement of the ith unit (locomotive or rake); k_i and d_i are the spring and damping constant of the coupler system; m_i and u_i are the mass and traction force of the ith unit, respectively; R^a and R^r are the aerodynamic and rolling resistances, respectively; θ_i is the slope angle, while degree of curvature is calculated as $D_i = 0.5d_{wheelbase}/R$, R being the curve radius. The gravitational and curvature resistance forces are $9.98m_i\sin(\theta_i)$ and $0.004m_iD_i$, respectively (Garg & Dukkipati, 1984).

The aerodynamic and rolling resistances are given as

$$R = \underbrace{c_0 + c_v v}_{R^r} + \underbrace{c_a v^2}_{R^a}, \tag{2}$$

where v is the velocity of the car, R^r is the rolling resistance, R^a is the aerodynamic drag and the coefficients c_0, c_v, c_a are obtained experimentally.

4. Controller design

4.1. Open-loop controller

The open-loop controller calculates the forces required for the train to maintain the desired speed under current conditions. Using the force equations in Section 3, the following results are obtained under the assumption that there is no acceleration and all cars are travelling at the same steady state velocity v_d:

$$\begin{aligned} u_1 = {} & k_1(x_1 - x_2) + (c_0 + c_v v_d)m_1 \\ & + c_a v_d^2 M + 9.98\sin\theta_1 m_1 + 0.004D_1 m_1, \end{aligned}$$

$$\begin{aligned} u_i = {} & k_i(x_i - x_{i+1}) - k_{i-1}(x_{i-1} - x_i) \\ & + (c_0 + c_v v_d)m_i + 9.98\sin\theta_i m_i \\ & + 0.004D_i m_i, \quad i = 2, \ldots, n-1, \end{aligned} \tag{3}$$

$$\begin{aligned} u_n = {} & -k_{n-1}(x_{n-1} - x_n) + (c_0 + c_v v_d)m_n \\ & + 9.98\sin\theta_n m_n + 0.004D_n m_n, \end{aligned}$$

where $M = \sum_{i=1}^{n} m_i$, v_d is the desired velocity.

The equations are under-determined in terms of variables $u_1, \ldots, u_n, x_1, \ldots, x_n$. Summing the equilibrium forces in Eq. (3), the total effective force required is

$$\begin{aligned} u_T & = u_1 + u_2 + \cdots + u_n \\ & = \sum_{i=1}^{n} m_i(c_a v_d^2 + c_0 + c_v v_d + 9.98\sin\theta_i \\ & \quad + 0.004D_i). \end{aligned} \tag{4}$$

There are no unique ways of distributing the forces $u_1, \ldots, u_n$ to satisfy Eq. (4). In this paper, it is assumed that in open-loop control the braking forces are all set to zero, and the required effective force u_T is equally distributed to the locomotives.

Once $u_1, \ldots, u_n$ are chosen according to Eq. (4), Eq. (3) can be used to uniquely determine $k_1(x_1 - x_2), k_2(x_2 - x_3), \ldots, k_{n-1}(x_{n-1} - x_n)$. If one takes the position of the leading car (usually a locomotive) x_1 as a reference, then in steady state, the relative positions (therefore, the in-train forces) are uniquely determined. These values are dependent on the traction forces of the locomotives, the braking forces of the wagons and the operation travelling speed.

4.2. Closed-loop controller

A closed-loop controller is designed based on a linearised system of the model described by force equation (1). A standard local linearisation procedure around a steady state of (1) results in the following state-space model:

$$\dot{\boldsymbol{x}} = \begin{bmatrix} \mathbf{0}_{n\times n} & \mathbf{I}_{n\times n} \\ \mathbf{A}_{21} & \mathbf{A}_{22} \end{bmatrix} \boldsymbol{x} + \begin{bmatrix} \mathbf{0}_{n\times n} \\ \mathbf{B}_{21} \end{bmatrix} \boldsymbol{u}, \tag{5}$$

where

$$\mathbf{B}_{21} = \mathbf{I}_{n\times n}, \tag{6}$$

$$\mathbf{A}_{21} = \begin{bmatrix} -\frac{k_1}{m_1} & \frac{k_1}{m_1} & 0 & \ldots & 0 & 0 & 0 \\ \frac{k_1}{m_2} & -\frac{k_1+k_2}{m_2} & \frac{k_2}{m_2} & \ldots & 0 & 0 & 0 \\ \vdots & \vdots & \vdots & \ddots & \vdots & \vdots & \vdots \\ 0 & 0 & 0 & \ldots & \frac{k_{n-2}}{m_{n-1}} & -\frac{k_{n-2}+k_{n-1}}{m_{n-1}} & \frac{k_{n-1}}{m_{n-1}} \\ 0 & 0 & 0 & \ldots & 0 & \frac{k_{n-1}}{m_n} & \frac{-k_{n-1}}{m_n} \end{bmatrix}, \tag{7}$$

$$\mathbf{A}_{22} = \begin{bmatrix} -c_v - \frac{2c_a v_d M}{m_1} & 0 & \ldots & 0 \\ 0 & -c_v & \ldots & 0 \\ \vdots & \vdots & \ddots & \vdots \\ 0 & 0 & \ldots & -c_v \end{bmatrix}. \tag{8}$$

The state variables $\boldsymbol{x} = [\delta x_1 \ \cdots \ \delta x_n \ \delta\dot{x}_1 \ \cdots \ \delta\dot{x}_n]$ and $\boldsymbol{u} = [\delta u_1 \ \ldots \ \delta u_n]$ are the deviations from the steady states obtained by solving the open-loop controller.

4.3. Fencing

The state-space term $\mathbf{B}_{21}$ in Eq. (6) assumes individual control for each car. In practice this is usually not possible. The main constraint is the availability of robust control signal bandwidth.

Currently on the COALlink of Spoornet, the train consists of 200 wagons. One ECP brake signal for all wagons and two control signals for the two locomotive groups, four locomotives at the front and two at the rear, are used. This is the control configuration that is called a unified control configuration.

In the unified control configuration, for a train setup with a locomotive at the front of the train with four wagons, the state-space term $\mathbf{B}_{21}$ is, for example,

$$\mathbf{B}_{21} = \begin{bmatrix} 1 & 0 \\ 0 & 1 \\ 0 & 1 \\ 0 & 1 \\ 0 & 1 \end{bmatrix}.$$

By taking advantage of individual braking capabilities offered by the ECP system, while keeping within the control signal bandwidth constraint, a concept of adaptive wagon fencing is proposed.

The idea of adaptive wagon fencing can be explained with the help of Figs. 1 and 2. In Fig. 1, with unified brake signal, car 6 has to apply its brake although it is on an uphill. Instead of using six signals for individual control, adaptive wagon fencing requires three, shown in Fig. 2. Car 6 is now coasting. Wagons experiencing similar track conditions are controlled as a group. The term fence refers to the separation of the control signals.

The adaptive wagon fencing controller automatically calculates new fences for the train as it travels down the track

$$F = [f_1, f_2, \ldots, f_j], \tag{9}$$

where f_j is the first car after the fence, i.e., control signal separator. For example, the fence in Fig. 2 would be $F = [2, 3, 6]$. The number of fences j varies with the complexity of the track modulation the whole train experiences. The state-space term $\mathbf{B}_{21}$ will also change as

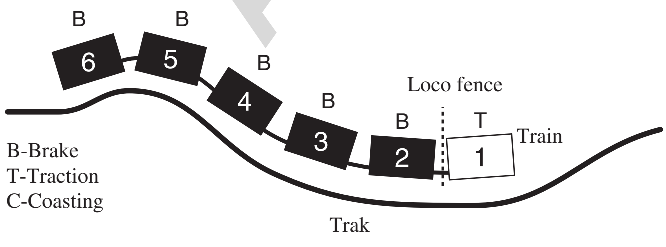

Fig. 1. Train control with only one control signal for all wagons.

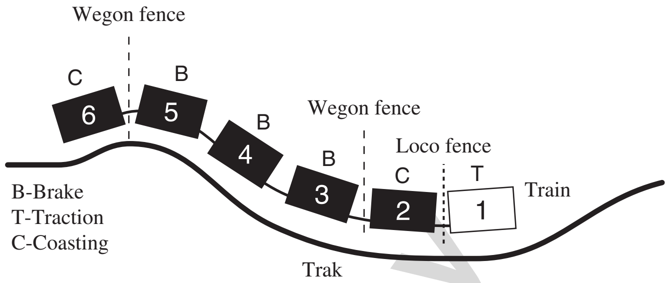

Fig. 2. Train control with adaptive fence.

a new fence is being generated

$$\mathbf{B}_{21} = \begin{bmatrix} \mathbf{1}_{f_1-1} & \mathbf{0}_{f_1-1} & \cdots & \mathbf{0}_{f_{j-2}-1} & \mathbf{0}_{f_j-1} \\ & \mathbf{1}_{f_2-f_1} & \cdots & & \\ & & \cdots & \mathbf{1}_{f_{j-1}-f_{j-2}} & \\ \mathbf{0}_{n-f_1+1} & \mathbf{0}_{n-f_2+1} & \cdots & \mathbf{0}_{n-f_{j-1}+1} & \mathbf{1}_{n-f_j+1} \end{bmatrix},$$

where $\mathbf{0}_i$ and $\mathbf{1}_i$ denote column vectors of 0 and 1 of length i, respectively.

The concept of adaptive fencing is well related to the interest in the control community in reconfigurable/switching control systems (Wu, 1995).

To evaluate whether a new set of fences is required, the controller calculates the median of the slope angles and the track curvature the train experiences at each sampling time t_s. If either the new slope median or track curvature median exceeds the previous value by a predefined threshold f_{th}, the controller will calculate a new set of fences.

From the leading car, the controller will add a fence between the current and the next unit (locomotive or rake) under the following conditions:

(i) The unit type differs, e.g., rake following a locomotive.
(ii) The slope experienced by the next unit exceeds the slope experienced by the previous fenced unit by a predefined threshold f_{seg}.
(iii) The above condition occurs for the track curvature.

4.4. LQR control

Based on the LQR optimisation method described in Goodwin, Graebe, and Salgado (2001), the cost function is defined as

$$J = \int_0^\infty (\mathbf{x}'\mathbf{Q}\mathbf{x} + \mathbf{u}'\mathbf{R}\mathbf{u})\,\mathrm{d}\tau, \tag{10}$$

where $\mathbf{Q}$ and $\mathbf{R}$ are the weights.

To use the LQR method, the running costs: in-train force, fuel consumption and travelling time, need to be quantified. Fuel consumption is the simplest to tackle, as it is directly related to u. Thus, the diagonal of the gain matrix R will determine the fuel consumption as well as brake usage, i.e.,

$$\mathbf{R} = \begin{bmatrix} r_1 & 0 & \dots & 0 \\ 0 & r_2 & \dots & 0 \\ \vdots & \vdots & \ddots & \vdots \\ 0 & 0 & \dots & r_n \end{bmatrix}, \tag{11}$$

where $r_i, i = 1, \dots, n$, are the weighting coefficients for the traction and brake force on each car. In cases of unified control and adaptive fencing, size n will change accordingly.

The weighting matrix Q is chosen so that

$$\begin{aligned} \delta\mathbf{x}'\mathbf{Q}\delta\mathbf{x} = \sum_{i=1}^{n-1} & q_{1i}k_i^2(\delta x_i - \delta x_{i+1})^2 \\ & + q_{1i}d_i^2(\delta\dot{x}_i - \delta\dot{x}_{i+1})^2 \\ & + \sum_{i=1}^{n} q_{2i}(\delta\dot{x}_i - v_d)^2, \end{aligned}$$

in which all the q's are positive. The term q_{1i} is to penalise the in-train forces experienced by the couplers, and the term q_{2i} is to penalise the travelling speed tracking of the whole train.

To bring the three weights to the same magnitude, weights $\mathbf{R}$ and q_{2i}'s are multiplied by the maximum of the k_i.

Although the closed-loop controller will not be able to optimise the travelling time and fuel efficiency at the global level, i.e., for the full length of the track, through coefficients q_{2i} and r_i travelling time and fuel consumption can be optimised locally, i.e., at the current track position. Thus all three cost factors of a heavy-haul train, i.e., travelling time, fuel consumption and in-train force, are quantified into tunable parameters in the LQR controller.

A closed-loop LQR controller takes the form

$$\mathbf{u} = K\mathbf{x}.$$

The overall controller consists of the open-loop controller, added to the closed-loop controller.

5. Results

Train parameters from the companion paper (Chou et al., 2006) are used. Other parameters are shown in Table 1. A particularly difficult track on the COALlink line is used. According to specifications, the maximum uphill grade allowed is $\frac{1}{160}$. In this section the maximum uphill grade is $\frac{1}{73}$. For this section the six locomotives will not be able to pull 200 wagons over the hill even at maximum traction if they operate without initial momentum. An experimental trial run on this section of track was conducted on the 18th November 2003. The train configuration is, four locomotives—200 wagons—two locomotives, from the front to the rear of the train.

Table 1
Heavy-haul train parameters

Parameter	Value	Unit
No. of wagons	200	
No. of locomotives	6	
Simulation time	2000	s
Sampling time	0.1–10	s
Faulty locomotive position	4th	
Input offset	−1.5	km
Initial position	12	km
Initial velocity	10	ms^{-1}
Initial altitude	1920	m

5.1. Open-loop and closed-loop control

In the first set of simulations, a unified control configuration is assumed. Simulated on a validated model with real track conditions, the controller performance results are very close to what is obtainable from actual trains.

In the trial run, the reference velocity was not recorded. From the data, it seems the reference was generally kept constant. For the simulation, additional changes to the reference velocity are added to demonstrate the controller's reaction to reference changes.

The open-loop controller is able to follow the reference velocity very slowly, as shown in Fig. 3, reaching the average reference. As expected, steady-state errors are present.

For the generic closed-loop controller, q_{1i} and q_{2i} are set to 1. Shown in Fig. 4, the generic closed-loop controller is able to track the reference very closely. The deviations around 71–75 km are caused by the uphill slope previously mentioned.

5.2. Parameter tuning

The generic controller in Fig. 4 is optimised slightly for velocity tracking, although the weights q_{1i}, q_{2i} and r_i are all set to 1. Referring to Section 4.4, by changing the weights q_{1i} and q_{2i} to 59 and 0.1, respectively, the controller is tuned to put the emphasis on minimising in-train forces. Similarly, by adjusting q_{2i} and r_i values to 0.1 and 12, respectively, more emphasis is placed on energy efficiency. Finally, to put more emphasis on velocity tracking, q_{2i} values are set to 12.

Fig. 5 shows the simulated output of a velocity regulation emphasised controller. The four graphs reflect the velocity of the first locomotive, the in-train force of the front coupler of the first wagon, the control signal and the track height, respectively. The first two graphs compare the velocity and in-train force, V_{sim} and F_{sim}, with their respective counterparts, V_{w4} and F_{w4}, that were recorded on the experimental trial run. Similar graphs for in-train force and energy emphasised controllers are shown in Figs. 6 and 7, respectively.

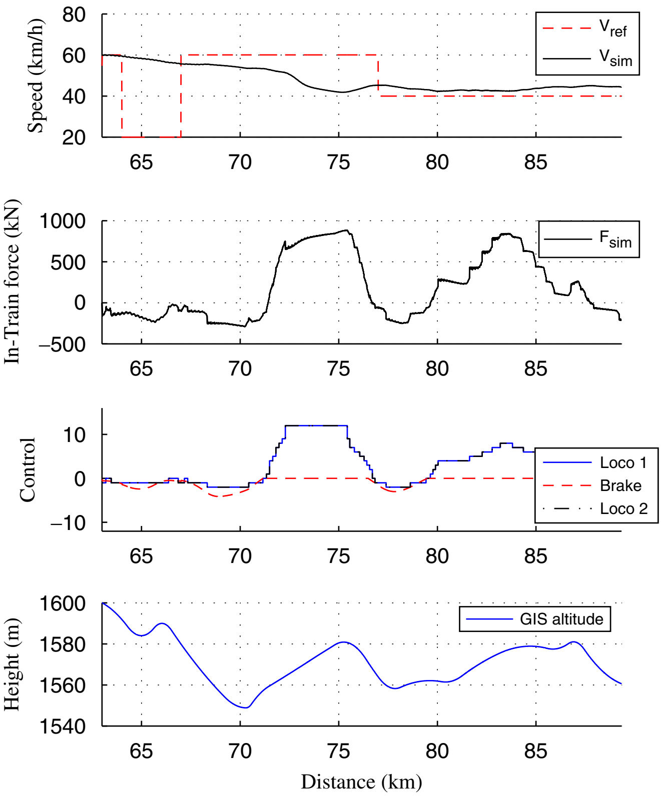

Fig. 3. Open-loop controller result.

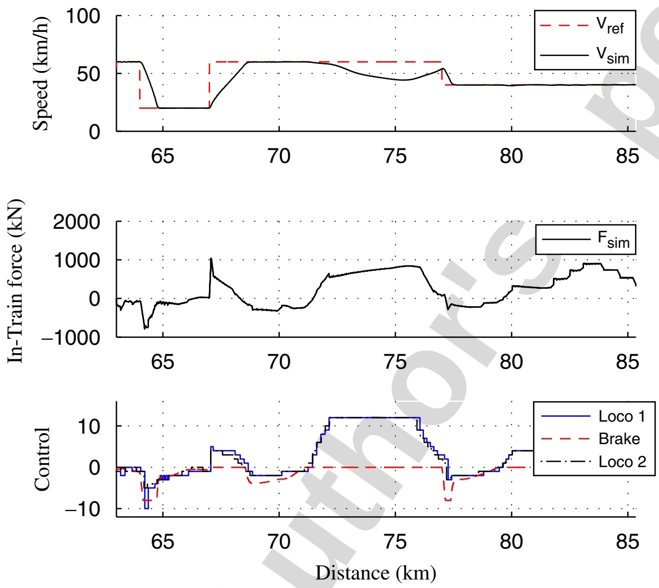

Fig. 4. Closed-loop controller: generic tuning parameters.

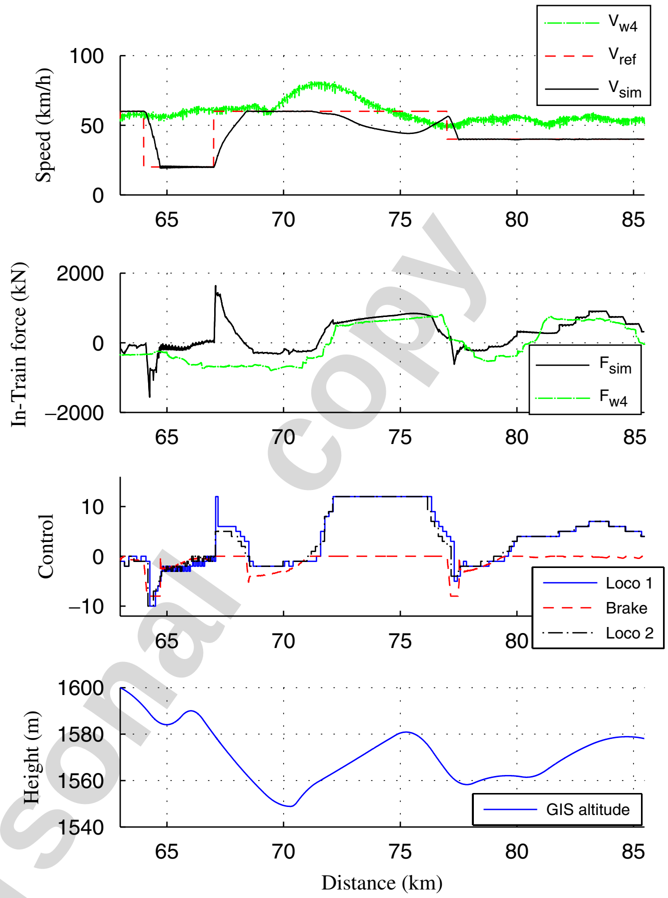

Fig. 5. Closed-loop controller optimised for velocity tracking.

Comparing Figs. 5 and 4, the largest difference lies in the two large in-train force peaks at 63 and 67 km in the second graph. This worsening of in-train force handling is the result of the improvement in velocity regulation.

Comparing Figs. 6 and 7 to Fig. 4, the results show the major differences. The top graph of each figure shows the velocity output. For energy and in-train force emphasised controllers, velocity tracking is gentler, resulting in smoother and slightly slower transitions. The second graph of each figure shows the in-train forces at the coupler before the first wagon, where the highest in-train force usually occurs. For both energy and in-train force emphasised controller, large in-train forces are reduced, specifically the two large peaks at 63 and 67 km. Traction and braking usage is greatly reduced, again from 63 to 67 km and at 77 km. The link between large traction usage and large in-train force is evident.

Table 2 records the simulated values of various important performance indices, such as velocity deviation from the reference velocity. Comparing values for the energy and in-train force emphasised controllers to the values for the generic controller again shows similar overall improvement. However, direct comparison between the energy emphasised controller and the in-train force emphasised controller would be unjustified owing to lack of common ground.

While energy optimised and in-train force optimised controllers give similar results, velocity tracking optimised controllers show the other end of the spectrum. From both Fig. 5 and Table 2, it is clear that improvement in velocity tracking sacrifices in-train force and energy usage, where the maximum in-train force is nearly doubled.

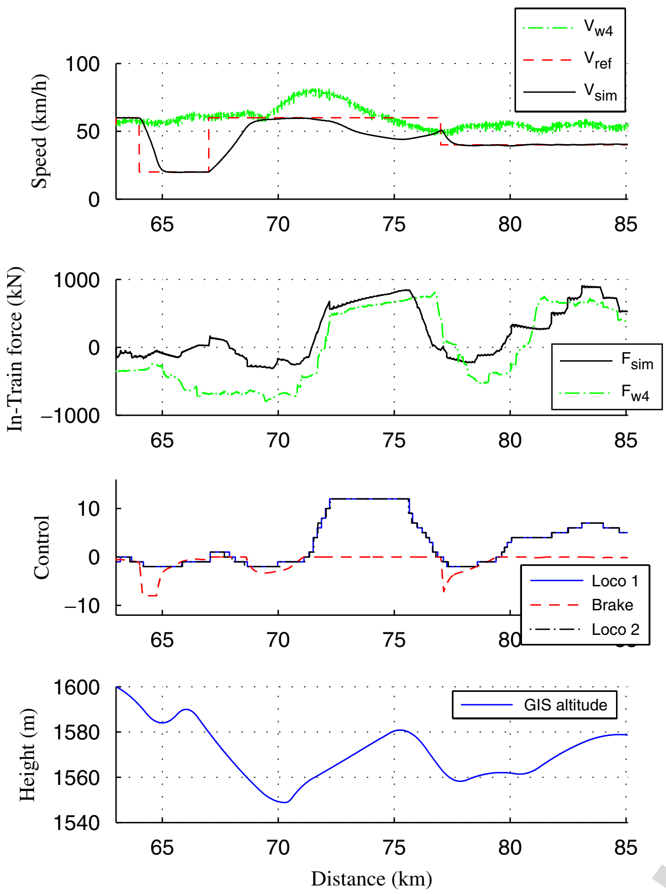

Fig. 6. Closed-loop controller optimised for in-train force.

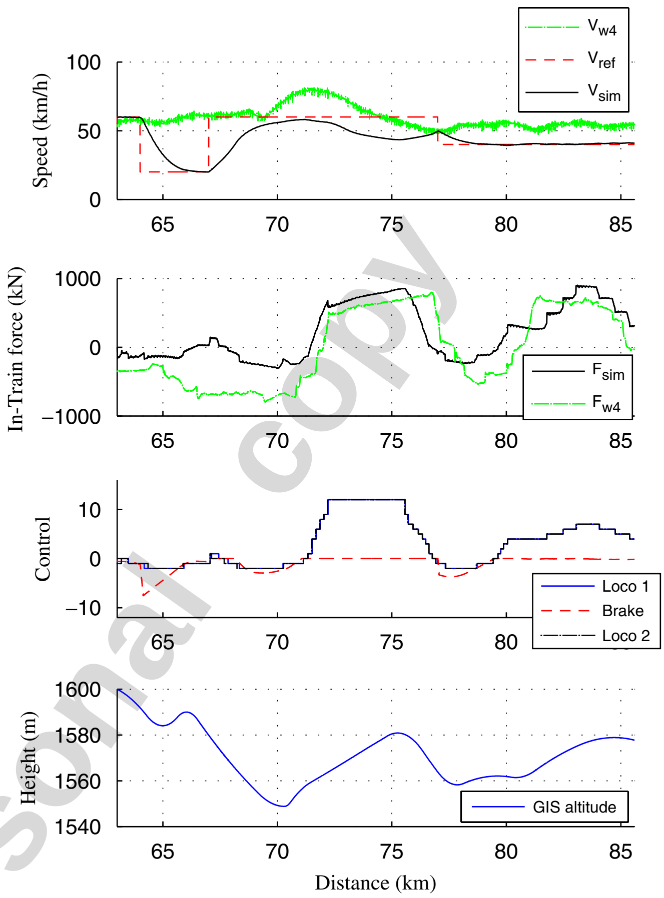

Fig. 7. Closed-loop controller optimised for energy usage.

5.3. *Adaptive wagon fencing versus full individual control*

In this comparison threshold values f_{th} and f_{seg} of 2×10^{-4} and 1×10^{-4} for slope angle, and 1×10^{-4} and 5×10^{-5} for curvature are used. Weights q_{1i} and q_{2i} of 12 and 3 are used, respectively. These parameters are not optimally tuned.

Referring to Section 4.3, adaptive fencing is the proposed control method to utilise the additional available control channels to improve the operation efficiency.

Table 3, similar to Table 2, compares the various performance indices between simulations. In this case, the different train configurations are compared. Unified control uses only one tractive and one brake control signal throughout the train, while adaptive fencing and individual control use more than one control signal.

From Table 3, it is clear that adaptive fencing is not able to reduce the in-train forces as well as individual control, even though both employ similar control actions. Further comparisons of Figs. 8 and 9 confirm this. Examining the in-train forces in both graphs shows that full individual control is able to reduce the peak in-train forces further at 63 and 67 km. However, both adaptive fencing and individual control are able to reduce tractive energy consumption.

Table 2
Performance indices for in-train force emphasised, velocity emphasised and energy usage emphasised controllers

Current value	In-train forces	Velocity tracking
Vel. deviation: Absolute mean (km/h)	6.8767	4.9946
Mean (km/h)	−4.5972	−2.9909
In-train force: Minimum (kN)	−309.4605	−1562.6711
Maximum (kN)	843.6625	1640.8775
Energy usage: Traction (MJ)	536.051	682.77
Dynamic braking (MJ)	−119.9479	−190.4987
Current value	**Energy usage**	**Generic**
Vel. deviation: Absolute mean (km/h)	8.6896	5.4804
Mean (km/h)	−4.6265	−3.4834
In-train force: Minimum (kN)	−304.03	−788.8906
Maximum (kN)	854.5669	1041.2118
Energy usage: Traction (MJ)	537.9416	620.9923
Dynamic braking (MJ)	−132.5898	−157.1676

6. Conclusion

This paper completes the two part study on heavy-haul train control. The controller is adaptive for different optimisation objectives: energy consumption, velocity

Table 3
Comparison of the performance indices between adaptive fencing and full individual control

	Unified control	Adaptv. Fencing	Full indiv.
Velocity deviation			
Absolute mean (km/h)	4.9409	5.2289	6.2383
Mean (km/h)	−3.1756	−3.4494	−3.636
Static in-train force			
Min. (kN)	−550.3345	−480.3234	−312.179
Max. (kN)	842.2614	911.342	902.7567
Energy consumption			
Traction (MJ)	926.2305	896.7763	870.7232
Dynamic braking (MJ)	−130.5269	−137.8525	−138.8401

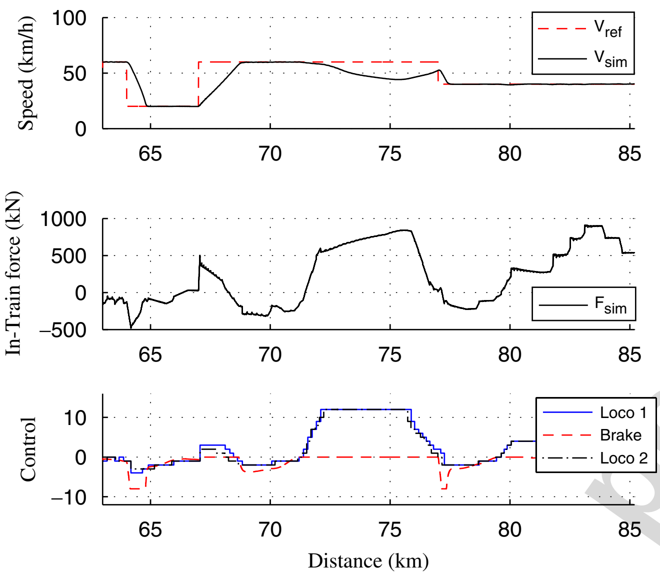

Fig. 8. Closed-loop controller optimised with fencing group control.

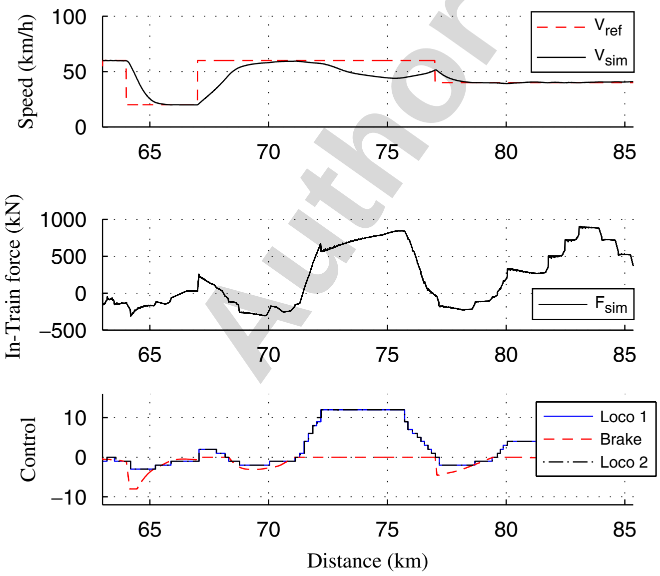

Fig. 9. Closed-loop controller optimised for full individual control.

tracking and in-train force. When implemented, this would allow drivers to change the optimisation objectives with respect to the current track condition. For example, velocity tracking could outweigh energy consumption when a train is late for shipment.

From the results, it is clear that by emphasising in-train forces, the controller will provide overall operational improvements. It also shows that large in-train forces are associated with large control actions. Adaptive fence control requires further refinement in fence positions before achieving the performance of full individual control, but to keep the bandwidth constraint, this is perhaps the price that one has to pay.

The robustness of the LQR closed-loop controller is guaranteed as long as the parameters are set in their proper ranges (Lin & Olbrot, 1996). In application, train parameters are entered into the system during the initialisation stage. This reconfigures the controller for that particular train for both performance and robustness.

It can be stated that the proposed cruise controller has achieved its goal. To implement the controller, the full state variable information must be available. The feasibility of sensors and observers is under current investigation. With further testing and tuning, the implementation of such controllers is possible in the foreseeable future. This would allow the reduction on the fourth category of running cost of heavy-haul trains: the human workload.

It is also noted that the techniques of this paper are linear, based on linearised models around the operation points. Both speed controllers and braking controllers are implemented by taking into consideration the nonlinearities, especially during the acceleration period. The "optimal" setting, as outlined in this paper, needs to be taken as a rough initial solution.

References

AAR (2002). *Manual of standards and recommended practices, electronically controlled brake system.* Technical Report, Association of American Railroads.

Astolfi, A., & Menini, L. (2002). Input/output decoupling problems for high speed trains. *Proceedings of the American control conference* (pp. 549–554).

Chou, M., Xia, X., & Kayser, C. (2006). Modelling and model validation of heavy-haul trains equipped with electronically controlled pneumatic brake systems. *Control Engineering Practice*, in press, doi:10.1016/j.conengprac.2006.09.006.

Garg, V. K., & Dukkipati, R. V. (1984). *Dynamics of railway vehicle systems* (xiii ed.). Toronto: Academic Press.

Goodall, R. M., & Kortum, W. (2002). Mechatronic developments for railway vehicles of the future. *Control Engineering Practice*, *10*, 887–898.

Goodwin, G. C., Graebe, S. F., & Salgado, M. E. (2001). *Control system design*. New Jersey: Prentice-Hall.

Gruber, P., & Bayoumi, M. M. (1982). Suboptimal control strategies for multilocomotive powered trains. *IEEE Transaction on Automatic Control*, *27*(3), 536–546.

Hawthorne, M. J. (2003). Real world benefits from electronic train control technologies. *Heavy haul conference*, Dallas, May 2003.

Howlett, P. (1996). Optimal strategies for the control of a train. *Automatica*, *32*(4), 519–532.

Howlett, P. G., Milroy, I. P., & Pudney, P. J. (1994). Energy-efficient train control. *Control Engineering Practice*, *2*, 193–200.

Ishikawa, Y., & Kawamura, A. (1997). Maximum adhesive force control in super high speed trains. *Proceedings of the power conversion conference* (pp. 951–954), Nagaoka, Vol. 2.

Khmelnitsky, E. (2000). On an optimal control problem of train operation. *IEEE Transaction of Automatic Control*, *45*(7), 1257–1266.

Kull, R. C. (2001). Wabtec ECP system update. *Proceedings of the 2001 IEEE/ASME joint railroad conference* (pp. 129–134).

Lin, F. & Olbrot, A. W. (1996). An LQR approach to robust control of linear systems with uncertain parameters. *Proceedings of the 35th conference in Decision and control* (pp. 4159–4163).

Mei, T. X., Nagy, Z., Goodall, R. M., & Wickens, A. H. (2002). Mechatronic solutions for high-speed railway vehicles. *Control Engineering Practice*, *10*, 1023–1028.

Pearson, J. T., Goodall, R. M., Mei, T. X., & Himmelstein, G. (2004). Active stability control strategies for a high speed bogie. *Control Engineering Practice*, *12*, 1381–1391.

Perez, J., Busturia, J. M., & Goodall, R. M. (2002). Control strategies for active steering of bogie-based railway vehicles. *Control Engineering Practice*, *10*, 1005–1012.

Tang, T., & Gao, C. (1996). A new train speed automatic control system for the Chinese railway. *Proceedings of the IEEE international conference on industrial technology* (pp. 76–79).

Thelen, G. A., & Tse, Y. H. (1990). An automatic speed enforcement system for heavy freight trains. *Railroad conference* (pp. 31–39).

Watanabe, T., & Yamashita, M. (2001). A novel anti-slip control without speed sensor for electric railway vehicles. *The 27th annual conference of the IEEE industrial electronics society*, Vol. 2, pp. 1382–1387.

Wu, N. (1995). Control design for reconfigurability. *Proceedings of the American control conference* (pp. 102–106).

Yang, C. D., & Sun, Y. P. (2001). Mixed H_2/H_∞ cruise controller design for high speed trains. *International Journal of Control*, *74*(9), 905–920.